

Surface-tension suppression of lamellar swelling on solid substrates

V.A. Parsegian *, R. Podgornik ¹

Laboratory of Structural Biology, Division of Computer Research and Technology and Office of the Director of Intramural Research/NIDDK, National Institutes of Health, Bethesda, MD 20892, USA

Received 2 December 1996

Abstract

Multilayers of charged lipids immersed in distilled water swell to whatever dilution allowed them by the available volume of solvent. Multilayers of the same lipids on a solid surface will imbibe only a small amount of water from a vapor, even from a 100% relative-humidity vapor. We argue that the essential difference is in the extra work needed to create a vapor/multilayer interface. For stiff, tightly packed multilayers, this interfacial energy is an additive constant of little consequence. But, in liquid water, multilayers swell to a softness where thermal excitation creates a rippled surface; the surface energy goes as the contour area not as the flat area of projected surface. The contour area grows as the multilayer swells. Vapor/liquid surface tension creates a “hard” surface that quells ripples and, usually, pulls the multilayer back to tighter packing. Tension can act to enhance direct attractive bilayer–bilayer forces such as weak van der Waals interactions to create new energy minima at very close spacings. These new energy minima might explain the limited swelling of charged lipids on substrates. What is remarkable is the long range and the strength of surface-tension perturbation on layered systems. In our statistical-thermodynamic formulation, bilayer motion is treated as the sum of undulations or waves that can pervade the entire multilayer. Disturbance of the surface can reach inward to distances comparable to the lateral extent of the multilayers. We use measured osmotic compressibility and bending rigidity to reveal the qualitative difference in affinity for water of multilayers in liquids and those on substrates exposed to vapors of the same chemical potential. © 1997 Elsevier Science B.V.

1. Introduction

Two different models of “smectic” systems ([1–3]) have argued that in lamellar multilayers there is a “mechanical van der Waals force” acting to suppress swelling of systems bounded by high energy surfaces. The idea is that the membranes will necessarily undulate in highly swollen multilayers. Any undulation of the surface layer necessarily creates a contour surface area greater than that of a stiff flat layer [3]. A surface tension or

additional work needed to create or to stiffen the air/multilayer surface will necessarily increase the cost of creating such undulations; their magnitude will be suppressed compared to what will occur without that surface perturbation.

The remarkable and surprising result of recent formulations is that this suppression can extend into the multilayer far from the layer at the surface. One immediate consequence of this extended suppression is that multilayers will not swell as much as they could when their surfaces are free to move. The action of a high energy bounding surface might even explain the qualitative difference in multilayer swelling in liquid solution vs in vapors, the “vapor pressure paradox” ([3]).

* Corresponding author.

¹ On leave from J. Stefan Institute, Ljubljana, Slovenia.

It has been a long-neglected question why charged bilayers, for example, immersed in distilled water will take up essentially infinite amounts of water ([4,5]): the same bilayers adsorbed to a solid surface will imbibe only a small amount of water from a 100% relative-humidity vapor ([6,7]). Neutral melted-chain phosphatidylcholines will take up to ~ 50 wt% water from the liquid ([8,9]) but will accumulate only 30 wt% from a 100% r.h. vapor ([6,7,10]). Even for lipids in a frozen-chain “gel” phase, there is a qualitatively different response to liquid vs vapor even though the water is applied at the same chemical potential ([11]).

We have now found a way to connect the multilayer spacing w to be seen in a substrate-deposited multilayer with the surface energy γ that acts at the multilayer/vapor interface. We compare this bilayer repeat spacing w with the larger one found for multilayers of the same lipid material but immersed in solution and subject to the same osmotic stress of water.

We make this connection by using a thermodynamic formalism by focusing on the thermally driven undulations that occur throughout a multilayer made of a finite number of layers adsorbed to a solid surface. We look in particular at those motions that are sensitive to changes in surface tension between the top-most layer and the medium – vapor or liquid. The multilayer bending energy and compressibility perpendicular to the layers that determine the magnitude of these undulations are extracted from osmotic stress measurements on multilayers in solution. It is possible to construct a parallel between the traditional Laplace hydrostatic pressure on a curved surface and a dehydration pressure on a surface whose roughness is due to thermally driven undulation.

By working through two sets of calculations based on actual experimental systems, we attempt to establish a rational basis for systematic further measurement. The product of the bilayer bending stiffness and the multilayer compressibility modulus is key to the sensitivity a multilayer will show to surface tension. Softer systems undergo larger surface undulations which, in turn, become more costly and unlikely with high surface tension. Because of the way surface and bulk energies are coupled in layered systems, most systems will pay

the price of compressing the stack of layers in order to smooth the surface layer and lower their surface energy.

2. Method

It is easiest to understand the free energy G of a multilayer, adsorbed to a solid surface (Fig. 1) and exposed to a vapor, via its dependence on two pertinent variables: Π_{osm} , the applied osmotic stress, and γ , the surface energy per area between the multilayer and the vapor above it.

We think about changes $dG(\Pi_{osm}, \gamma)$ in free energy as,

$$dG(\Pi_{osm}, \gamma) = \left. \frac{\partial G}{\partial \Pi_{osm}} \right|_{\gamma} d\Pi_{osm} + \left. \frac{\partial G}{\partial \gamma} \right|_{\Pi_{osm}} d\gamma \quad (1)$$

The coefficient $(\partial G)/(\partial \Pi_{osm})|_{\gamma}$ has units of volume and is, specifically, the volume of water

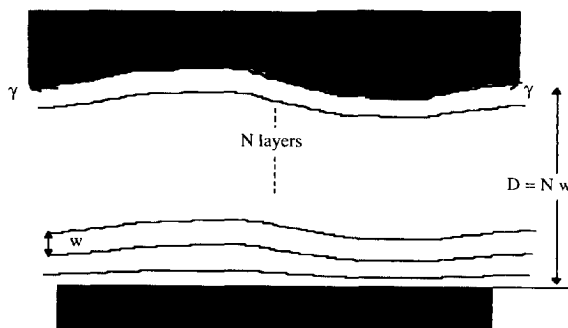


Fig. 1. Multilayer of N layers adsorbed onto a solid substrate and exposed to water vapor. The mean spacing between layers is w so that the total thickness of water in the multilayer is $D = Nw$. For mathematical brevity, the thickness of the bilayer itself is treated as zero. The activity of the vapor is expressed in terms of equivalent osmotic stress, Π_{osm} . (A change $d\Pi_{osm}$ in osmotic stress is related to the change in the chemical potential of water $d\mu_{water}$ by a factor $-v_w$, $d\mu_{water} = -v_w d\Pi_{osm}$, where v_w is the molecular (or molar) volume of water. The equivalent osmotic stress is related to the relative humidity p/p_o by $\Pi_{osm} = -(kT/v_w) \ln(p/p_o)$.) The surface tension γ acts only on the topmost (mono)layer, exposed to the vapor. Computed energies will be given per unit area projected on the (flat) substrate. (In the Appendix A, the full multilayer is taken as having lateral dimensions of $L \times L$ rather than the section shown here.) The surface energy goes as the rippled, contour area with a surface energy density γ . Undulatory modes are those degrees of freedom allowed to the whole sample.

$V_w = V_w(\Pi_{osm}, \gamma)$ that can be added or removed either under osmotic stress or by surface-tension restriction of undulations; $(\partial G)/(\partial \gamma)|_{\Pi_{osm}}$ has units of area, specifically the full area of the vapor-exposed multilayer surface².

$$dG(\Pi_{osm}, \gamma) = V_w(\Pi_{osm}, \gamma) d\Pi_{osm} + A_{total}(\Pi_{osm}, \gamma) d\gamma \quad (2)$$

This area A_{total} is the sum of L^2 , the projected flat area of the multilayer, and the extra area due to rippling. L^2 is constant. The contour area depends on applied stress and tension; it is crucially interesting to the vapor suppression of swelling. The lateral extent L is much greater than thickness D . For present purposes, it can be imagined as having an indefinitely large value. We will concentrate therefore on the relative excess area $A_c = A_c(\Pi_{osm}, \gamma)$. This is the difference between the total area, A_{total} , and projected area, L^2 , divided by L^2 . A_c is the excess, contour area per unit projected area.

$$A_c = (A_{total} - L^2)/L^2 \quad (3)$$

This definition allows us to concentrate on that part of the surface that changes with tension. From this point on we treat the free energy $G(\Pi_{osm}, \gamma)$ as per unit projected, flat area.

Since the order of differentiation doesn't matter, the cross derivatives in $G(\Pi_{osm}, \gamma)$ are equal.

$$\frac{\partial^2 G}{\partial \Pi_{osm} \partial \gamma} = \frac{\partial^2 G}{\partial \gamma \partial \Pi_{osm}} \quad (4)$$

This identity allows us to create an instructive relation between the sensitivity of area $A_c(\Pi_{osm}, \gamma)$ to osmotic pressure and the sensitivity of water volume $V_w(\Pi_{osm}, \gamma)$ to tension γ .

$$\left. \frac{\partial V_w}{\partial \gamma} \right|_{\Pi_{osm}} = \left. \frac{\partial A_c}{\partial \Pi_{osm}} \right|_{\gamma} \quad (5)$$

² It would be a happier world if the signs in front of the V_w and A_{total} terms were obvious. They should be here. Nevertheless some comment might be helpful. The free energy G is to be considered the work of creating the multilayer. Any increase in the energy of γ of exposed surface A_{total} will necessary increase the cost of creating that surface. Similarly if a volume of water V_w has been collected and the osmotic squeezing force Π_{osm} has been increased, then there is an increase in the work needed to collect that volume.

This Maxwell cross-relation shows the balance between surface and volume work. If a multilayer is stiffened by an increased osmotic stress, the amplitude of the undulatory surface is decreased. Conversely, if there is an increase in the tension on those undulations, the volume of water in the undulation-swollen bilayer will change.

That part of the multilayer area that depends on surface tension γ is (Appendix A, Eqs. (A29) and (A30),

$$\begin{aligned} \left. \frac{\partial G}{\partial \gamma} \right|_{\Pi_{osm}} &= +A_c(\Pi_{osm}, \gamma) \quad (6) \\ &= \frac{kT}{8\pi} \frac{q_{Max}^2}{\sqrt{K_c B} + \gamma} + \frac{kT}{8\pi D K_c} \\ &\quad \times \frac{\ln\left(\frac{1 + \gamma/\sqrt{K_c B}}{2}\right)}{1 - (\gamma/\sqrt{K_c B})^2} \approx \frac{kT}{8\pi} \frac{q_{Max}^2}{\sqrt{K_c B} + \gamma} \end{aligned}$$

D is the total thickness of water in the multilayer, N layers \times water spacing w . B is the compressibility modulus, $B(w) = -w(\partial \Pi_{osm}/\partial w)$; K_c is the per-volume bending modulus k_c/w where k_c is the bending modulus of a single layer (Appendix A, Eqs. (A2) and (A3)). (For succinctness, the actual physical thickness of the bilayer is taken to be zero; this thickness does not change detectably under low osmotic stress conditions to be considered here ([12, 8, 13]).

2.1. Sensitivity of repeat spacing to surface energy

Because osmotic stress measurements on multilayers are calibrated to measurements of repeat spacing to total water volume ([8]), we use the approximation $V_w \approx Nw$ omitting explicit dependence of water volume V_w on contour area. The instability of a multilayer subject to surface tension γ is discussed as the sensitivity of water spacing w to changes in γ . We re-write the Maxwell relation Eq. (5) as

$$\left. \frac{\partial V_w}{\partial \gamma} \right|_{\Pi} = N \left. \frac{\partial w}{\partial \gamma} \right|_{\Pi} = \left. \frac{\partial A_c}{\partial \Pi} \right|_{\gamma} \quad (7)$$

This relation gives the change in w with γ as,

$$\frac{\partial w}{\partial \gamma} \Big|_{\Pi_{osm}} = - \frac{kT}{8\pi N} \frac{q_{Max}^2}{(\sqrt{K_c B} + \gamma)^2} \frac{\partial \sqrt{K_c B}}{\partial \Pi_{osm}} \Big|_g \quad (8)$$

Since $\sqrt{K_c B} = \sqrt{K_c(w)B(w)}$ is a material property built from osmotic stress measurements on multilayers in liquids, it and its Π_{osm} derivative are taken as a bulk property independent of γ . $\sqrt{K_c(w)B(w)}$ appears as a kind of natural unit of γ .

In X-ray scattering from lamellar systems this $\sqrt{K_c(w)B(w)}$ is used as a disorder parameter as first suggested by Caillé [14]. It is used to describe the shape of X-ray diffraction peaks when layers undulate (see also Refs. [10], [15], [16] and [17]).

3. Results

We examine the swelling pressure, structure and packing energies of two different kinds of lipids whose material properties have been measured in solutions with osmotic stress. Those material properties will be introduced into expressions for multilayers immobilized onto a solid substrate and exposed to a vapor that not only sets the chemical potential of the water but also creates a tension γ at the vapor/multilayer interface. In this case, the multilayer is between the “rock” of the substrate and the progressively “harder place” of a surface under tension. Our source data are the osmotic stress vs water spacings measured for typical phospholipids in solution (e.g. [8,9]).

There are limited data on the spacing of lipids immobilized on substrates but immersed in liquid water rather than vapor. One report [18], on phosphatidylcholine in this condition, states that the multilayer swells to the same spacings that it shows when completely immersed in water (although after days the lipid disperses into the excess-water bath). We will use this information to say that the zero-tension “ $\gamma=0$ ” situation here is for a material that has the same properties as lipid in bulk water. (Since we are looking mainly at changes in multilayer spacing with changes in γ , this assumption about the $\gamma=0$ reference state is probably not critical.)

Computations are for a 30-ångstrom cutoff wave vector, $q_{Max} = 2\pi/30 \text{ \AA}$. This minimum wavelength

is chosen to be comparable to the bilayer thickness. This choice is to ensure that a continuum model is used only for the mesoscopic dimensions of bilayer structure. A different q_{Max} would change the magnitude of estimated fluctuations but would not change the qualitative nature of the response to γ . We work with multilayers of $N=100$ layers. For present purposes, parameters used are to be considered illustrative only. The individual bilayer bending elasticity coefficient is taken to be $k_c = 25kT = 10^{-12} \text{ erg}$ [19].

3.1. Phosphatidylcholine (PC) multilayers on a solid substrate, tension-induced contraction

For a typical zwitterionic melted-chain phosphatidylcholine in solution there is an exponential repulsive force $\Pi_0 e^{-w/\lambda_h}$, with $\Pi_0 = 10^{10.6} \text{ erg cm}^{-3}$ and $\lambda_h = 2.1 \text{ \AA}$ ([8] Table 1) which works against a van der Waals attraction. Here, this van der Waals force/area is given the form for the interaction between planar layers of thickness t , separation w :

$$P_{vdw}(w) = \frac{A_{Ham}}{6\pi} \left[\frac{1}{w^3} - \frac{2}{(w+t)^3} + \frac{1}{(w+2t)^3} \right]$$

With a Hamaker “constant” of $6 \times 10^{-14} \text{ erg}$ and a hydrocarbon thickness $t=30 \text{ \AA}$ ([8] Table 1; [20]), this attractive pressure balances the hydration exponential at $w \sim 26 \text{ \AA}$ under zero osmotic stress where it creates an energy minimum $\sim 0.01 \text{ erg cm}^{-2}$ deep ([21]).

The pressure vs spacing is shown in Fig. 2 where attraction and repulsion balance at approximately 26.3 \AA .

The compressibility modulus $B(w) \equiv -w(\partial \Pi_{osm} / \partial w)$, Fig. 3, maintains an exponential dependence to a separation significantly larger than the repulsive range of $\Pi(w)$. It changes sign at a separation of about 30.4 \AA , 4 \AA more than the position for the zero in pressure.

At the same time, the disorder or Caillé parameter ([14]) $\sqrt{K_c(w)B(w)}$ drops monotonically to zero near $d=30 \text{ \AA}$. (Fig. 4) This function has units of surface tension. Formally it always appears as a ratio $\gamma/\sqrt{K_c B}$ or a sum $\sqrt{K_c B} + \gamma$. It is a natural unit for measuring the importance of surface energy. For this reason, we expect significant sur-

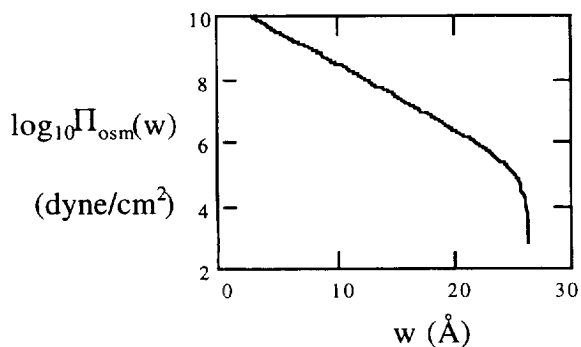


Fig. 2. Osmotic stress Π_{osc} measured on neutral phosphatidylcholine multilayers in solution. The stress as plotted here uses a form fitted to the data rather than the data points themselves. This fitted form will be used to derive multilayer compressibility $B(w) = -w(\partial\Pi_{osc}/\partial w)$ as well as to compute the response of the material to surface-tension perturbation. The fitted osmotic pressure curve approaches a minimum at $\sim 26 \text{ \AA}$, the result of balancing exponential repulsion and power-law attraction.

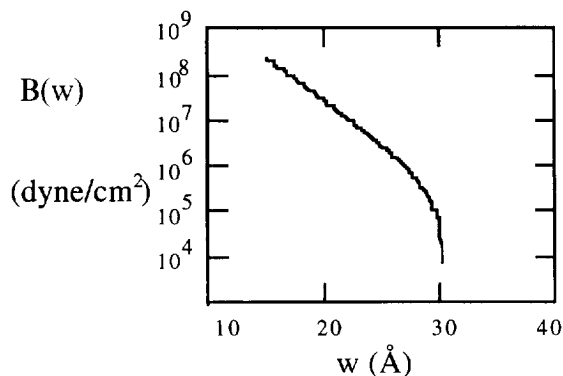


Fig. 3. Multilayer compressibility derived from osmotic stress, $B(w) = -w(\partial\Pi_{osc}/\partial w)$. Note the shift in the location of the minimum to near 30 \AA separation.

face tension perturbation for those separations where γ is comparable to or greater than $\sqrt{K_c(w)B(w)}$.

To within an additive constant, the energy of interaction $E(w)$ is the integral of osmotic stress vs separation. We choose the zero of energy at infinite separation, $E(w \rightarrow \infty) = 0$. In the case of zero surface tension, there is a weak “secondary” minimum at $\sim 26 \text{ \AA}$ separation where forces balance (Figs. 2 and 5).

The material properties, $B(w)$, $K_c(w) = k_c/w$, and $\Pi(w)$, from bilayers in solution, are used to esti-

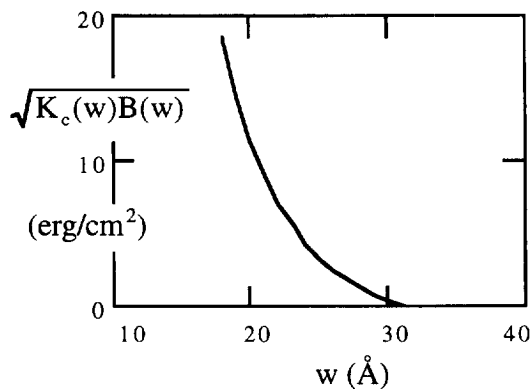


Fig. 4. The disorder parameter $\sqrt{k_c(w)B(w)}$ at different bilayer separations. This quantity, also known as the Caillé parameter ([14]). Large values correspond to stiff multilayers that give sharp X-ray scattering peaks. Small values, near positions of force balance, suggest disorder in the multilayer lattice.

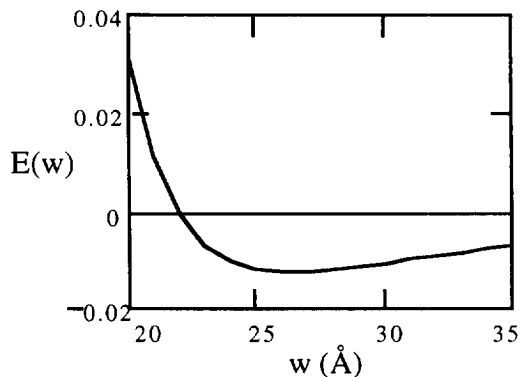


Fig. 5. The energy of interaction $E(w)$ per area between adjacent bilayers. The “zero” of this energy is in the limit of large separation. This is an energy per pair of bilayers. The total energy of the multilayer is $NE(w)$. Later, addition of surface energy will be shown as upward shifts in each part of this curve.

mate the excess surface area due to undulation under the stress of different surface energies γ . By Eq. (cc), the excess area per unit projected area of multilayer, is (Section 2, Eq. (6)),

$$A_c(\Pi_{osc}, \gamma) = A_c(\Pi_{osc}(w), \gamma) = \frac{kT}{8\pi} \frac{q_{Max}^2}{\sqrt{K_c B} + \gamma}$$

With progressive loosening of the lattice, at small pressures $\Pi_{osc}(w)$, there are greater undulations in the surface. These undulations are quelled by the cost γ of creating an interface. This quelling

is apparent in the downward shift from the “ $\gamma = 0$ ” line to the lines for 1, 10 and 100 erg cm⁻² in Fig. 6.

Because of undulations, a finite γ increases the energy needed to create a multilayer of given spacing w . Think of taking the value of energy $E(d)$ at $\gamma=0$ and adding energy in increments $A_c(d,\gamma)d\gamma$ while maintaining constant w and $\sqrt{K_c(w)B(w)}$. The additional energy is $\int_0^\gamma A_c(d,\gamma) d\gamma$ per unit area due to surface undulation. (We omit the energy γ of the flat surface since it is constant in w ; we need look only at factors that change the energy of swelling as a function of separation.) The total energy per layer is a sum,

$$E_{\text{total}}(w) = E(w) + \frac{kTq_{\text{Max}}^2}{8\pi N} \int_0^\gamma \frac{d\gamma}{\sqrt{K_c B} + \gamma}$$

$$= E(w) + \frac{kTq_{\text{Max}}^2}{8\pi N} \ln \left(1 + \frac{\gamma}{\sqrt{K_c B}} \right) \quad (10)$$

The number of layers, N , is in the denominator of the surface-energy term because $E(w)$ and

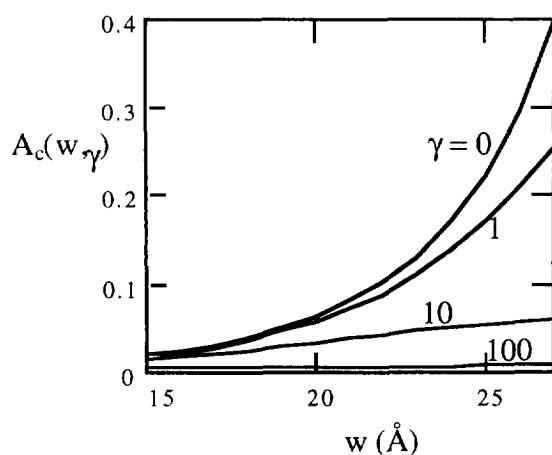


Fig. 6. The rippled, contour area $A_c(\Pi_{\text{osm}}(w), \gamma)$ at different water-layer spacings and applied tensions, $\gamma=1, 10$ and 100 dyn cm^{-1} . As plotted, this area is dimensionless since it is the excess area divided by the flat, projected area occupied by the multilayer on the substrate. It can also be thought of as an excess area of undulation per unit area of substrate. Application of surface tension dramatically suppresses undulatory area, especially at the larger spacings where multilayers are highly compressible.

$E_{\text{total}}(w)$ are expressed as energies per layer in a stack of N layers.

The effect of this additional energy is to create an energy minimum at a different position from that without surface energies. There is, physically, an attractive force created by the surface tension. Swollen multilayers cost more surface energy. The action of surface tension then is to pull the layers together. This shift in the energy vs distance curve is shown in Fig. 7 for $\gamma=0, 1, 10$ and 100 erg cm^{-2} .

Computed at constant applied osmotic stress, Π_{osmotic} , rather than under the constant-spacing condition used to compute $E_{\text{total}}(w)$, the repeat spacing varies with change in surface tension γ (Section 2, Eq. (8)):

$$\frac{\partial w}{\partial \gamma} \Big|_{\Pi_{\text{osm}}} = - \frac{kT}{8\pi N} \frac{q_{\text{Max}}^2}{(\sqrt{K_c B} + \gamma)^2} \frac{\partial \sqrt{K_c B}}{\partial \Pi_{\text{osm}}} \Big|_{\gamma}$$

By evaluating this derivative at different spacings w and values of γ , one sees the pulling-in power of surface tension γ . The surface-energy cost of undulation is offset by stiffening the multilayer by compaction. There is a large response to γ when both $\sqrt{K_c B}$ and γ are small, that is when the multilayer is swollen and flexible. Fig. 8. Stiffening the stack either by moving to small w or by bringing it to high γ takes away the floppiness that confers sensitivity to changes in tension.

The process of pulling in can be seen in Fig. 9 which plots the repeat spacing w as a function of

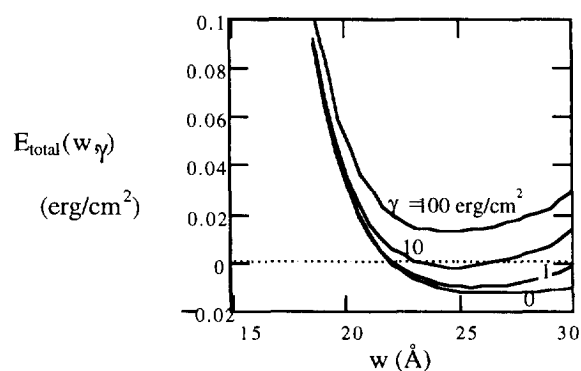


Fig. 7. Upward shift from $E(w) = E(w, \gamma=0)$ with application of surface tension. The extent of this shift is greater at the larger spacings where there is more motion in the loosely packed layers. The result is a shift in the effective energy minimum.

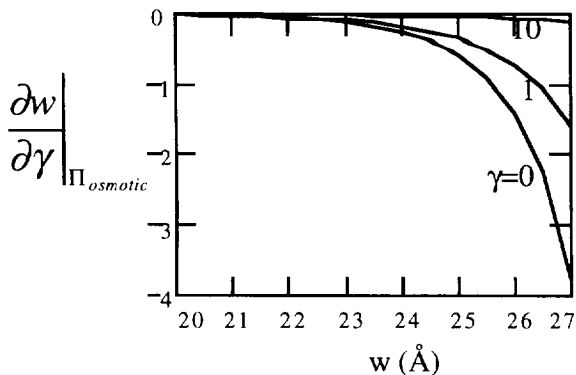


Fig. 8. Sensitivity of water spacing w to applied tension γ at constant osmotic stress. Multilayers are stiff at small spacings, refractory to surface perturbation. Near the $\sim 26 \text{ \AA}$ force-balance point, multilayers experience significant undulation and are thus susceptible to rising costs of creating contour area. The response to applied γ is to stiffen, to pay the osmotic price of compressing the layers rather than the price of larger surface energy. At high surface tension, 10 erg cm^{-2} for example, the multilayer is already stiff (having already been brought to that spacing by tension-induced compression) and there is little sensitivity to further increase in γ .

surface tension γ . In the present case, w decreases monotonically. There is maximum sensitivity to applied surface tension at low γ and at the wider spacings that go with low stress and high compressibility (Fig. 10).

It is now instructive to elaborate the initial plot of $\log_{10}(\Pi_{\text{osmotic}})$ vs zero-tension repeat spacing, $w = w(\gamma = 0)$, Fig. 2, to show the shift to $\log_{10}(\Pi_{\text{total}})$ vs repeat spacing $w = w(\gamma > 0)$ that occurs at each osmotic pressure. Here Π_{total} is the derivative of the energy per layer $E_{\text{total}}(w)$ and coincides with applied Π_{osmotic} at $\gamma = 0$.

On a linear P vs w plot, Fig. 11, it is possible to see the crossover between attractive and repulsive interlamellar force as it occurs at different surface tensions γ . The inset shows the shift in the position of maximum swelling, the minima of the energy $E_{\text{total}}(w; \gamma)$ vs separation d at each level of tension γ .

3.2. Phosphatidylserine (PS) multilayers on a solid substrate, tension-induced contraction and phase transition

Using osmotic stress force measurements ([5]) on phosphatidylserines (PS), we model the hydra-

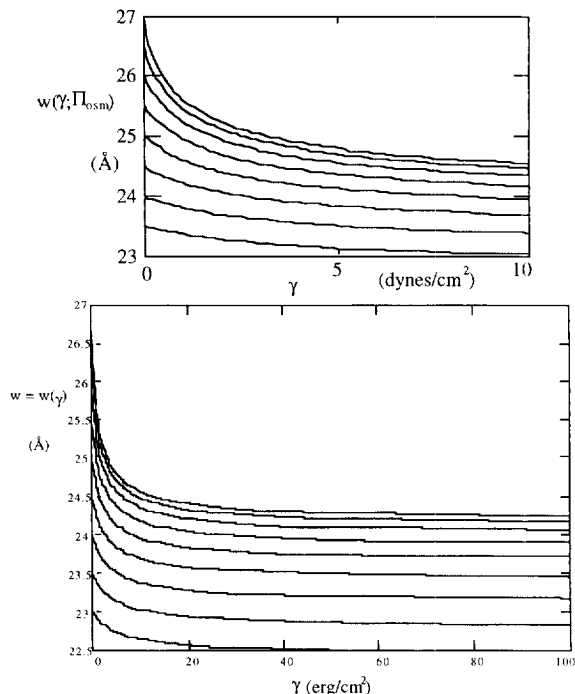


Fig. 9. Progressive pulling in of water spacing w as a continuous function of applied surface tension. The intercept with the vertical axis gives the spacing in the absence of surface tension, where bilayers have been brought to their respective separations only by osmotic stress. The computation is an iteration of the derivative $(\partial w)/(\partial \gamma)_{\Pi_{\text{osm}}}$ at each spacing w and corresponding osmotic stress $\Pi_{\text{osm}}(w)$. Change in w is most rapid at the smallest γ and goes to zero when tension reaches very high values.

tion force as equivalent to that between bilayers of phosphatidylethanolamine (PE), $P_h = 10^{12} \text{ erg cm}^{-3}$ with a decay constant $\lambda_h = 1.1 \text{ \AA}$. To this hydration force we add a van der Waals attraction for a finite slab of thickness t with a Hamaker coefficient of $8 \times 10^{-14} \text{ erg}$. These parameters gave an energy minimum of $\sim 0.1 \text{ erg cm}^{-2}$, similar to that measured by Evans and Needham ([21]) for PE. (We could have used a model with extra zwitterionic attraction ([22]) or one with hydration attraction ([23]), but the details of the different models will not concern us in the present illustration. We will keep with the simplest form for attractive forces.)

In addition to these PE interactions, in order to simulate electrically charged phosphatidylserine, we add an electrostatic double layer interaction

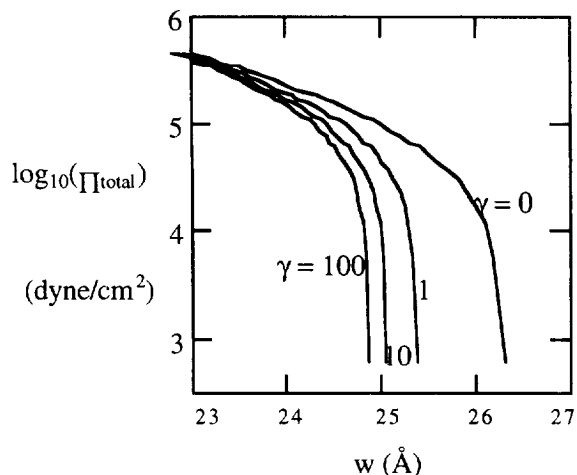


Fig. 10. Osmotic stress vs water spacing after the compressive effect of surface tension. The original data, Fig. 2, is shown as the $\gamma=0$ line. The $\gamma=1, 10, 100 \text{ dyn/cm}^{-1}$ curves are the result of the contraction portrayed in Fig. 9. The inward shift in the energy minimum, Fig. 7, now appears as a change in the position of effective force balance under the dual action of surface tension and forces within the multilayer.

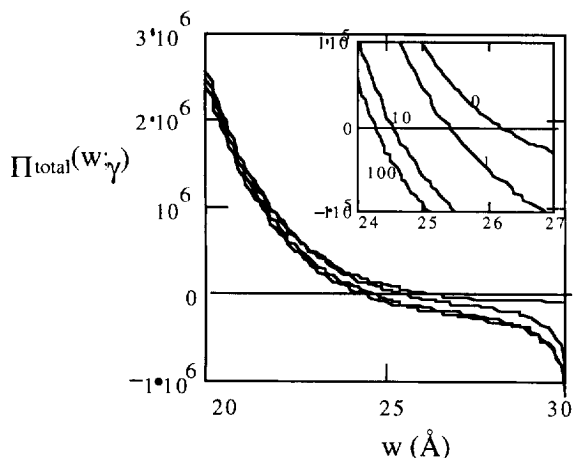


Fig. 11. Linear plot of apparent, "total" osmotic stress vs spacing, designed to show attractive forces that emerge with the application of surface tension. Inset: close-up to show shifts in force balance position. The appearance of attractive forces correspond to the creation of positive slopes in the energy vs spacing plots of Fig. 7.

$P_e e^{-w/\lambda_e}$, with coefficient $P_e = 5 \times 10^6 \text{ erg cm}^{-3}$ and a Debye decay length $\lambda_e = 10 \text{ \AA}$. The magnitude of this repulsion qualitatively follows that

seen in force measurement. Other forms of electrostatic repulsion will be treated in a later study.

As with PC, in the computations presented below the minimum wavelength of undulation is taken to be of the order of the phospholipid bilayer thickness, 30 \AA , to give a maximum wave vector $q_{\text{Max}} = (2\pi/30) \text{ \AA}^{-1}$. The bilayer bending elasticity coefficient is again $k_c = 25kT = 10^{-12} \text{ erg}$.

3.3. Pressure vs separation, no surface tension

The osmotic pressure Π_{osmotic} vs spacing d seen for surface-tension-free material shows the two dominant exponential regions — hydration and electrostatic double layer repulsion — that end with a drop-off around 65 \AA separation with the onset of the power-law attractive van der Waals force (solid line, Fig. 12). Because attractive forces will show an unexpectedly strong influence on the swelling of multilayers in the presence of surface tension γ , a plot of the interaction free of van der Waals attraction is also given in Fig. 12 (dotted line). Differences here on a $\Pi_{\text{osmotic}}(d)$ plot look small except near the $\sim 65 \text{ \AA}$ force-balance point.

Still, in the region between 19 and 23 \AA separation, there is a flattening in the slope that reflects the attractive force which created an energy minimum in the absence of electrostatic repulsion. The long-dashed line in Fig. 13 shows this minimum-energy position near 15 \AA separation for electri-

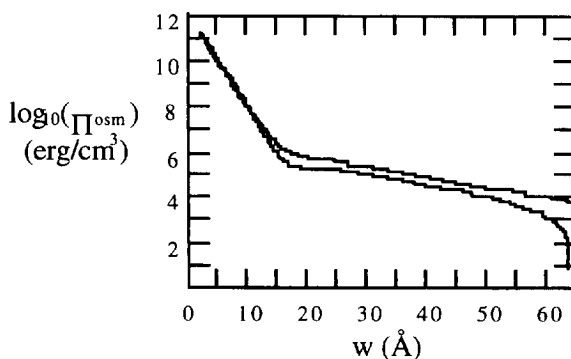


Fig. 12. Applied osmotic stress vs separation for charged bilayers in water (solid line). Dotted line, attractive force removed. The attractive force creates a force-balance position near 65 \AA . There is also a slight flattening of the stress with attractive forces in the separation between 15 and 30 \AA .

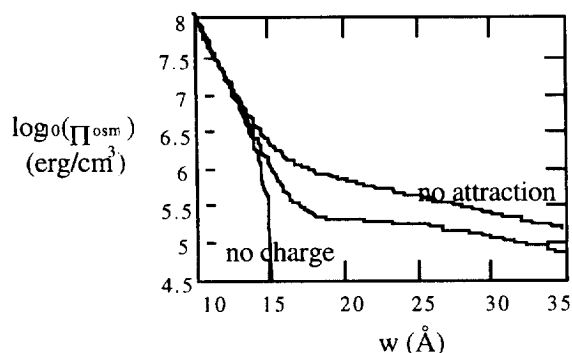


Fig. 13. Detail of osmotic stress vs separation to compare behavior with attractive force removed (dotted line) or electrostatic double layer force removed (dashed line). The absence of charged-bilayer repulsion creates a force balance at $\sim 15 \text{ \AA}$.

cally neutral bilayers, the separation where attractive van der Waals forces balance hydration repulsion.

3.4. Energy vs separation, no surface tension

The energy of interaction vs separation shows a very weak energy minimum where attraction balances repulsion near 65 \AA separation, but no minimum in the region of 19 to 23 \AA . This energy is taken here with respect to zero energy at infinite separation, the integral of $\Pi(w)$ measured in the absence of surface energy. It is the energy of interaction per pair of layers. The total energy of a stack of N layers is $NE(w)$ (Fig. 14).

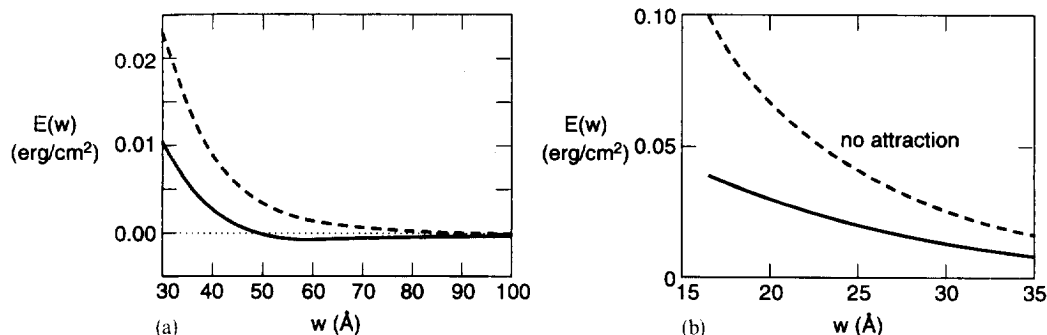


Fig. 14. Energy vs separation with respect to a zero at infinite separation. Solid line, hydration and electrostatic repulsion plus van der Waals attraction; dotted line, repulsion only. (a) Long range, energy minimum only at 65 \AA . (b) Short range, pure repulsion. These curves are interesting in part for their lack of feature.

3.5. Compressibility modulus $B(w)$ and fluctuation parameter $\sqrt{K_c(w)B(w)}$

The flattened region at $19 < w < 30 \text{ \AA}$ in $\Pi_{\text{osmotic}}(w)$ shows up as a wildly non-monotonic region in the compressibility modulus, $B(w) = w d\Pi/dw$. The extrema in this compressibility modulus (solid lines, Fig. 15) occur at 20.3 \AA for the minimum and 28.9 \AA at the maximum. The importance of the underlying attractive force in creating this non-monotonic behavior is clear from the dotted lines in Fig. 15 which are the compressibility modulus without the attractive force.

The non-monotonic behavior of $B(w)$, so clearly seen in Fig. 15, indicates a progressive hardening of the multilayer as it is compressed from the largest spacings but sudden softening below 30 \AA to a minimum value near 20 \AA . Further compression stiffens the multilayer again. All this occurs at the same time that there is only monotonically varying repulsion in the actual osmotic swelling pressure vs separation, Fig. 12. The attractive force “shows through” in the compressibility. Removal of attraction, dotted lines in Figs. 12 and 15, creates a monotonically stiffening compressibility modulus.

There is, from the same presence of significant underlying attractive forces in the 19 – 30 \AA range, a waxing and waning of the fluctuation parameter $\sqrt{K_c(w)B(w)}$ (Fig. 16). The minimum in $\sqrt{K_c(w)B(w)}$ near $w = 20 \text{ \AA}$ suggests that there is a softening of the multilayer there comparable to

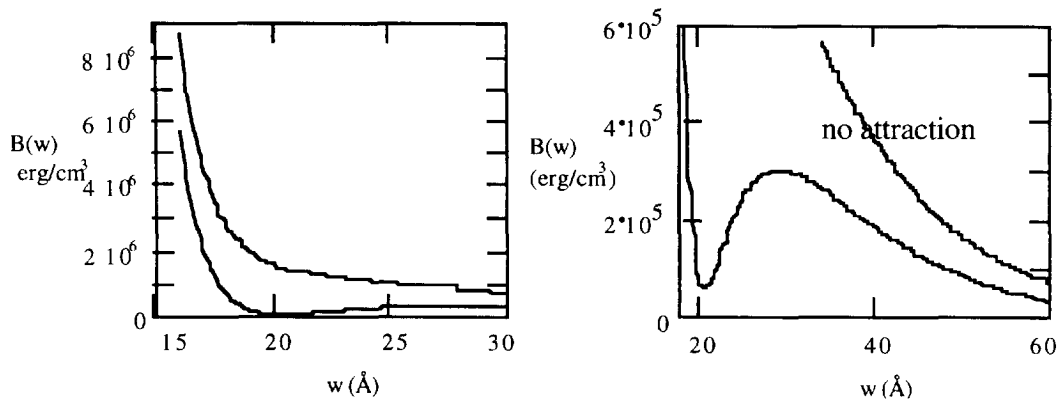


Fig. 15. The compressibility modulus shows strikingly non-monotonic behavior including a region of apparent multilayer stiffening with increasing separation from 20.3 to 28.9 Å. These features do not occur when attractive forces are absent (dotted lines). The derivative $w(\partial\Pi_{\text{osm}}/\partial w)$ creates a very different curve from its antecedent, Fig. 3 for PC multilayers.

that which occurs at separations greater than 40 Å where interaction forces are very weak. (The extrema here are at 20.3 Å for the minimum (as with B) and at 27.04 Å for the maximum.)

3.6. Excess undulatory area $A(w, \gamma)$, suppression by surface tension γ

There will be a comparable increase in undulatory fluctuations in this locally softened region, in fact an increase-then-decrease of undulatory excess area $A(w, \gamma)$ vs w . The maximum occurs at 20.3 Å and the minimum at 27 Å. Since the fluctuation

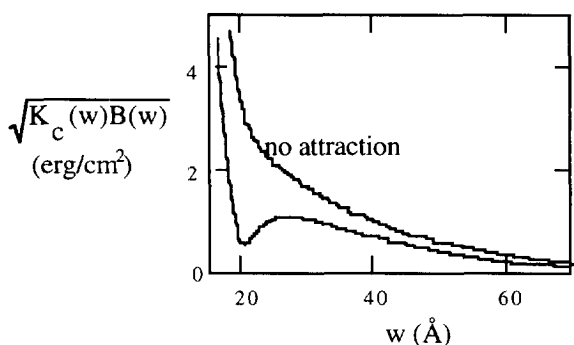


Fig. 16. Non-monotonic variation of disorder parameter vs water layer thickness. This variation suggests the existence of undulatory disorder in the multilayer in the region just above $w = 20$ Å.

parameter is $\sim 1 \text{ erg cm}^{-2}$ in the region of non-monotonic variation (Fig. 16), the excess area

$$A_c = \frac{kT}{8\pi} \frac{q_{\text{Max}}^2}{\sqrt{K_c B + \gamma}}$$

(Section 2, Eq. (6)) plotted in Fig. 17, is suppressed by the presence of relatively small surface energies $\gamma \sim 1 \text{ erg cm}^{-2}$. At small spacings, < 15 Å, there is only the expected monotonic increase in undulations with increasing spacing w .

To see the extent to which the wide variation in excess undulatory area $A_c(w, \gamma)$ reflects underlying attractive forces, we plot $A_c(w, \gamma)$ vs water spacing for the case where the attractive van der Waals force has been removed (Fig. 17(b)). The wide excursion in area is gone and replaced by a ripple from the switchover between hydration and electrostatic double layer forces near $w = 20$ Å.

3.7. Change in spacing with surface tension

The instability at 20.3 to 27 Å separations is more evident in the computed sensitivity of bilayer separation to interfacial tension,

$$\left. \frac{\partial w}{\partial \gamma} \right|_{\Pi_{\text{osm}}} = - \frac{kT}{8\pi N} \frac{q_{\text{Max}}^2}{(\sqrt{K_c B + \gamma})^2} \left. \frac{\partial \sqrt{K_c B}}{\partial \Pi_{\text{osm}}} \right|_{\gamma}$$

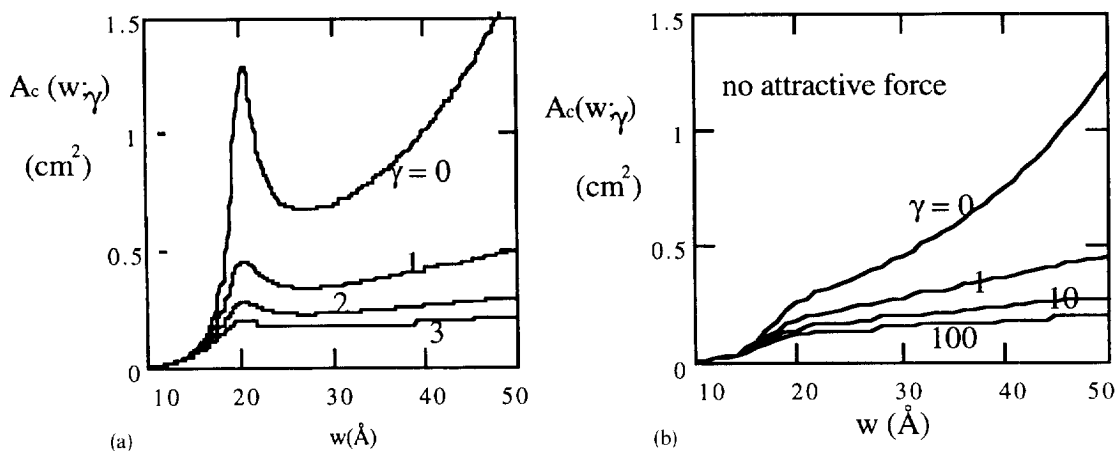


Fig. 17. Excess area, $A_c(w, \gamma)$, due to fluctuations of the multilayer surface. (a) Softening of the multilayer at separations around 20 Å creates a peak in undulatory surface area. Relatively small surface tensions – 1, 2, 3 dyn cm^{-1} – suffice to suppress undulations significantly. There is a range of separations, $w = 20.3$ to 27 Å, where the surface area decreases as a function of increasing separation. In this anomalous region, the effect of a finite tension will be to expand rather than to contract the multilayer. (b) No anomaly seen without attractive forces.

(Section 2, Eq. (8). The effect is, again, especially evident at very low tension (Fig. 18).

This down-and-up behavior suggests that there is a range of separations, 20.3 to 27 Ångstroms, at which $(\partial w)/(\partial \gamma)|_{\Pi_{osm}} > 0$ where the application of surface tension will actually drive multilayers to greater separations. There is a minimum in $\partial w/\partial \gamma|_{\Pi_{osm}}$ at 19.7 Å and a maximum at 20.9 Å

for the maximum. There are two points at which $(\partial w)/(\partial \gamma)|_{\Pi_{osm}} = 0$: 20.3 and 27 Å.

One can see the discrimination that occurs at these two separations by plotting the bilayer spacing vs applied tension (Fig. 19) while maintaining constant osmotic stress. Even at very low γ spacing w moves away from 20.3 Å. The spacing of 27 Å is a kind of gathering point, the application of

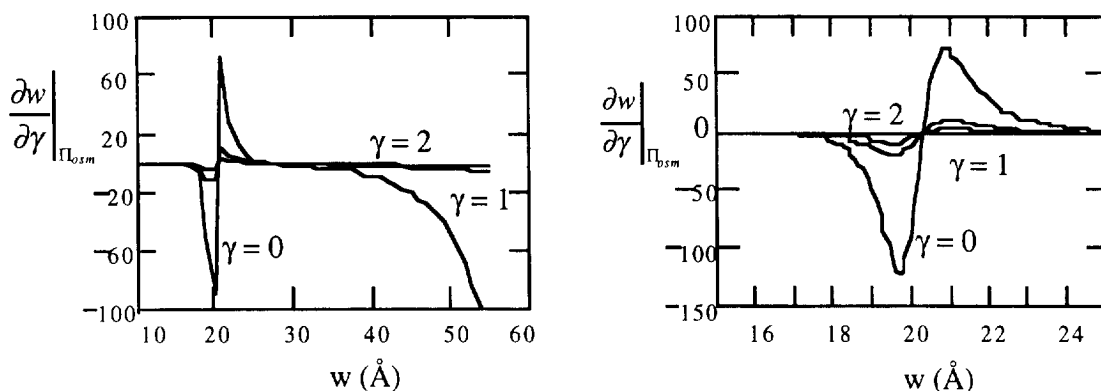


Fig. 18. Sensitivity of repeat spacing to applied tension. Each curve is for taking the derivative $\frac{\partial w}{\partial \gamma}|_{\Pi_{osm}}$ at the designated value of tension γ . It is especially important that there exists a region where this derivative is positive, where added tension is expected to increase the water spacing w . For separations initially just greater than 20.3 Å at $\gamma = 0$ the spacing will continue to grow until the derivative reaches zero (near 27 Å). Separations initially below 20.3 Å or greater than 27 Å will decrease with change in surface tension.

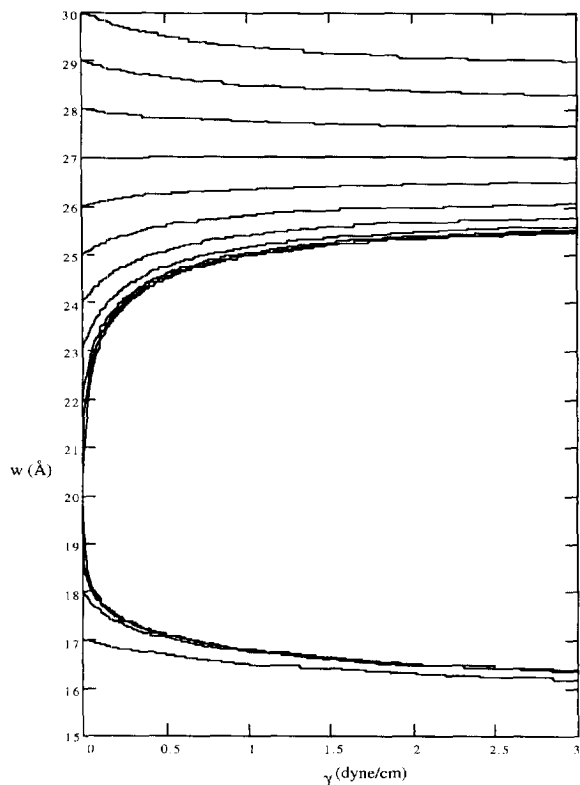


Fig. 19. Evolution of water spacings w as function of tension γ under application of constant osmotic stress. Points on vertical axis are those achieved under stress $\Pi_{\text{osm}}(w)$, see in solution, Fig. 12. The points to the right are those reached under applied γ . The separation from point 20.3 is almost immediate. The full consequence of finite γ is reached by $\sim 1 \text{ dyn cm}^{-1}$. Instability in spacings at zero tension is seen in the convergence of lines toward $w = 27 \text{ \AA}$ as well as away from $w = 20.3 \text{ \AA}$.

tension again causes multilayers to move toward this separation.

3.8. Pressure vs spacing, under surface tension

The nature of this instability around 20.3 and 27 Å becomes clear when we plot applied osmotic pressure vs spacing for multilayers under different applied surface tensions. Fig. 20 shows this for $\gamma = 1, 2$ and 3 erg cm^{-2} , together with the original Π vs w (from Figs. 12 and 13) at zero surface energy. With the application of small but finite tension, $\sim 1 \text{ dyn cm}^{-2}$, the $\log_{10}(\Pi)$ vs w curves cluster to nearly one curve with a jump in the region 16 to

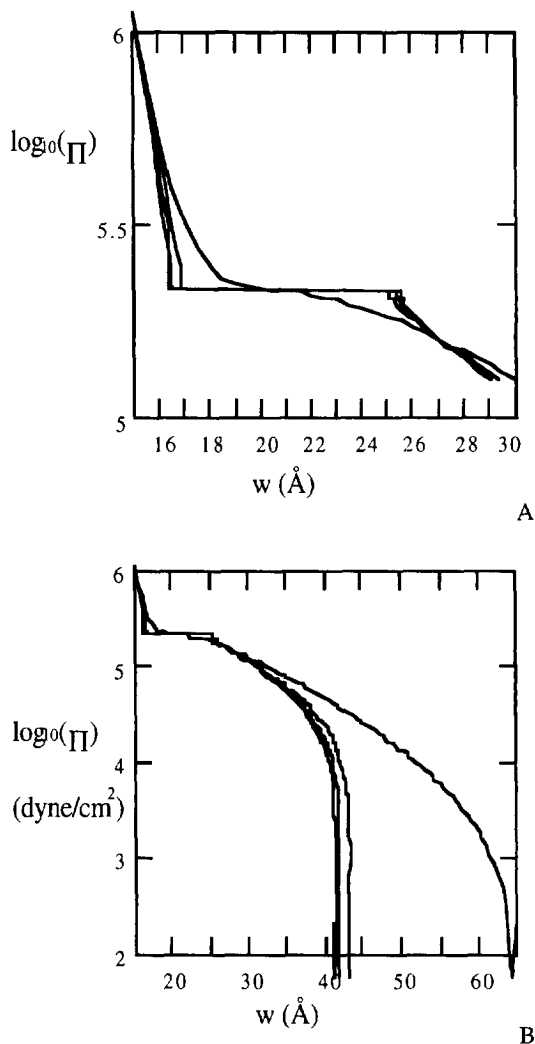


Fig. 20. Osmotic stress vs separation at $\gamma = 0, 1, 2$ and 3 dyn cm^{-1} . The clusterings and instabilities seen in Figs. 18 and 19 emerge here as horizontal tie-lines, effectively first-order transitions induced by added lateral stress on the surface. The horizontal break occurs about the 20.3 Å separation where a separation instability is seen above. The osmotic stress at this point is that of the initial $\Pi_{\text{osm}}(w = 20.3)$ measured in the absence of tension.

25 Å. This is the same region that showed an instability in Fig. 9 for $\partial w / \partial \gamma$ and in which, Fig. 19, tension was seen to drive the multilayer spacing away from the 20.3 Å separation point.

At much larger spacings, Fig. 20(B), applied tension pulls in the lattice from a force balance

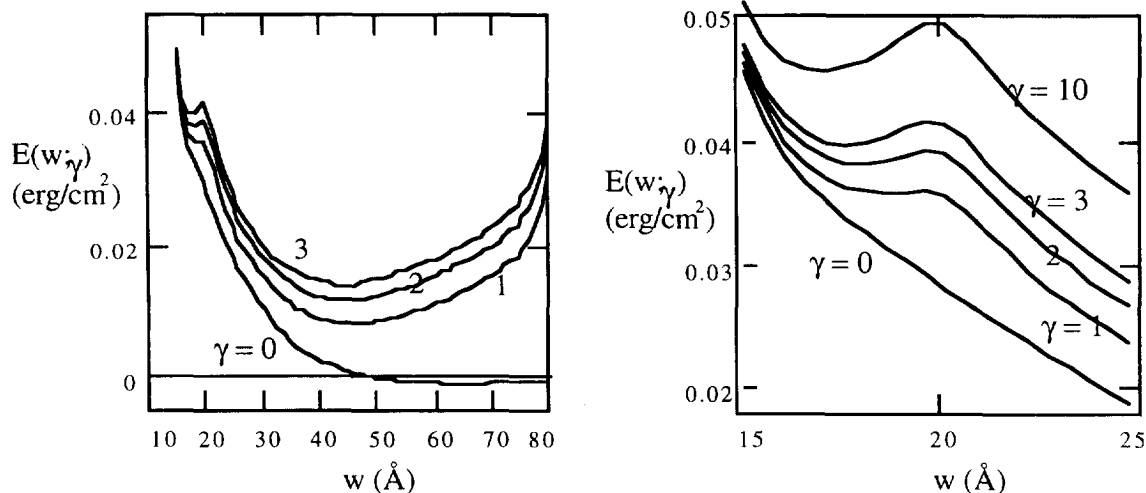


Fig. 21. Energy $E(w, \gamma)$ in the presence of applied tension. Points on the $\gamma = 0$ curve are shifted up by $\int_0^\gamma A_c(w, \gamma) d\gamma$. This shift, greater at spacings where multilayers are softer, creates local energy minima at small spacings.

point above 60 Å to one between 40 and 45 Å. It seems that very small surface tension suffice to induce contractions both at long and short range.

3.9. Interaction energy vs separation, under applied surface tension

The energy of interaction per unit area shows jumps and shifts in maxima and minima upon application of tension. These energies, plotted in Fig. 20, are taken with respect to a zero at infinite separation for the zero-tension multilayer. At each separation, w , there is an additional energy from integrating $\int_0^\gamma A_c(w, \gamma) d\gamma$ as described above. This additional energy, due to the work of creating an undulating surface, makes its greatest contributions when the multilayer is softest. These are the regions where the undulation parameter $\sqrt{K_c(w)B(w)}$, (Fig. 16), exhibits its smallest values. Comparison with Fig. 16 shows the expected minima in $\sqrt{K_c(w)B(w)}$ near $w = 20$ Å that turn into energy maxima here in Fig. 21.

4. Discussion

Why do lipid multilayers swell so differently when exposed to a vapor compared to their swell-

ing in liquids or in polymer solutions. The often-mentioned “paradox” is that water at the same chemical potential seems to be so differently accessible to the same material. Nowhere has this contradiction been seen more annoyingly than in the limited sorption of water by charged phospholipids deposited on solid substrates.

Our formulation/computation here suggests that the combined perturbations of substrate adsorption and of vapor/multilayer surface tension create the equivalent of attractive forces between layers. Bilayers are able to move in greatly swollen preparations. This movement itself is a force for swelling ([24]). Conversely, perturbations that stiffen the bilayers stifle swelling.

More interesting results occur when these “undulations” are coupled with direct long-range attractive and repulsive forces between layers. Repulsive forces are enhanced by the motion of bilayers ([25]); attractive forces are masked ([26]). The computations here suggest that surface-tension-suppression of undulation has a double effect: It weakens that part of observed repulsion that came from configurational entropy; it can reveal weak attractive forces that were previously overwhelmed by undulatory repulsion.

Two kinds of lipid system to illustrate these points.

(1) Substrate-deposited neutral “phosphatidylcholine” multilayers take up less water in vapor because surface undulations cost surface energy. The layers pull themselves tight even in the presence of small surface energies Figs. 7–11.

(2) Charged “phosphatidylserine” multilayers also pull together under surface tension. But they do much more. Even when there is a net repulsion for swelling in water, surface tension creates regions of net attractive force at small separation to prevent swelling in vapor, Fig. 20 These attractive forces occur in regions of local energy minima, Fig. 21 We argue below why it is easy for the multilayers to fall into the trap of these local minima and for charged lipids to fail to take up water in saturating vapors.

The reasons why surface tension can penetrate layered structures have been presented in an earlier paper ([3]). Intuitively, bilayer thermal motions can be resolved into independent degrees of freedom, undulatory modes whose longest wavelength are comparable to the lateral dimensions of the sample. Since these undulatory waves incur curvature and compressive energies they are three-dimensional events whose disturbance compresses the entire sample. Think of a drum-head. Any up/down displacement is communicated to the entire surface no matter its extent. The apparent wavelength of this distortion is as big as the diameter of the drum itself. When this drum is a “smectic” multilayer, the wave also compresses the stack and penetrates into the multilayer. Penetration depth is described as a parameter $1/a_q$ for each mode of wave vector $q = 2\pi/\lambda$ (Appendix A): λ is the wavelength whose largest dimension is that of the extent L of the multilayer domain; $a_q = \sqrt{K_c/B}q^2$ (Appendix A, Eq. (A10)); $1/a_q \sim \lambda^2 \sqrt{B/K_c}$ where B is a compressive stiffness and K_c is a bending stiffness. For $\lambda \sim L$, penetration into the multilayer goes as a length $L^2 \sqrt{B/K_c}$.

(3) Preparations with large domains L of coherent lamellar order will be perturbed to great depths by surface tension; small-domain preparations will not show strong surface effects.

(4) Multilayers that are hard to compress (big B) are expected to respond deeply to perturbations on the surface; but surface undulations are not

transmitted deeply into multilayers that already do not bend easily (big K_c).

Now add surface energy γ . The multilayer gauges γ in proportion to its material property $\sqrt{K_c}B$. Stiff materials, either in compression (large B) or bending stiffness (large K_c), do not feel additional surface effects. Undulations that would be suppressed by γ are already gone because the multilayer is inflexible. The parameter $\sqrt{K_c}(w)B(w)$ is key to designing experiments for examining the vapor pressure paradox. Preparations with small $\sqrt{K_c}B$ are those likely to show big differences when swollen in vapor rather than swollen in liquid.

To go further, consider the pressure vs separation and energy vs separation figures, Figs. 20 and 21. A charged bilayer that would move to a ~ 60 -Å spacing between bilayers in pure water will take up only 45-ångstroms of water in vapor. Even this much swelling is not seen in measurements (Jendrasiak et al., 1996). Rather, bilayers of this kind will take up only ~ 20 Å of water in near-saturating or saturating vapors. They seem to sit at the upper, local energy minimum near 18 Å shown in Fig. 21(b). According to the estimates of Fig. 20(a), an osmotic stress of $10^{5.5}$ erg cm^{-2} is needed to push these charged multilayers to this separation. This stress level is where one sees a flat region that has the appearance of a first-order transition.

What fluctuation in temperature is enough to lower the water vapor activity to deliver this level of stress? In terms of relative humidity, p/p_o the osmotic pressure is

$$\Pi_{\text{osmotic}} = -(kT/v_w) \ln(p/p_o) \approx -1.3 \times 10^9 \ln(p/p_o) \text{ erg cm}^{-3}$$

where $v_w = 30 \times 10^{-24}$ cm^3 , the volume of a water molecule and $kT = 4 \times 10^{-14}$ erg. The equivalent of $10^{5.5}$ erg cm^{-3} osmotic stress occurs at $\ln(p/p_o) = -10^{5.5}/1.3 \times 10^9 = -2.4 \times 10^{-4}$ or 99.98% relative humidity. The Handbook of Chemistry and Physics tells us that the vapor pressure of water changes by 2.69 kPa between 3.535 kPa at 300°C and 6.228 kPa at 310°C, an increase of 76%. The required change of 0.02% would require a temperature fluctuation of 0.003°.

Sorption of water through vapor by lipids is

very difficult to control. In osmotic stress measurements, it is usually good practice to work at 86% relative humidity or less ([27]). The form of the energy vs spacing profile near $w=20 \text{ \AA}$ in Fig. 21(b) suggests how a system may easily be trapped in a local minimum. In a saturating vapor, even in a super-saturating vapor, the surface energy remains a factor in swelling. To climb the $\sim 0.01 \text{ erg cm}^{-2}$ energy barrier shown in Fig. 21(b), even a 1 square micron patch would have to absorb $100 \text{ layers} \times (10^{-4} \text{ cm})^2 \times 0.01 \text{ erg cm}^{-2} \sim 10^{-8} \text{ erg}$, much more than thermal energy.

A profitable next step would be to examine the apparent first-order phase transition induced by surface tension, e.g. Fig. 20, in terms of a balance between surface and bulk energies. There is the equivalent of a Clausius–Clapeyron equation relating the tension and osmotic pressure at transition to the change in area and water volume.

$$\frac{d\Pi_{trans}}{d\gamma} = \frac{\Delta A_c}{\Delta V_w} \quad (12)$$

There is a first-order transition turned on by tension and even a kind of a critical point on a phase diagram at low tension.

There is also an intuitive connection to be developed between surface energy and internal osmotic stress similar to that between surface tension and hydrostatic pressure in the Laplace relation. There one speaks (for a sphere) of an energy change with change in surface area $\gamma d(4\pi r^2)$ balanced against the rate of change of energy with volume $p_L d(4\pi r^2/3) : \gamma 8\pi r dr = p_L 4\pi r^2 dr$ which gives the familiar relation $p_L = 2\gamma/r$.

Here, in our undulatory/osmotic case, one speaks of an energy from a change in area, $\gamma dA_c(w;\gamma)$, vs an energy change from a change in volume, $\Pi_\gamma d(Nw)$, per area of multilayer. (This Π_γ is an extra osmotic pressure due to the surface tension on top of what is supplied by external osmotic stress. The analogy with Laplace pressure is to see that there the pressure $p_L = 2\gamma/r$ is in addition to the background atmospheric pressure.) The two balancing changes in energy can be

parameterized as functions of spacing w :

$$\gamma \left. \frac{\partial A_c}{\partial w} \right|_\gamma dw = - \frac{kT}{8\pi} \frac{q_{\text{Max}}^2}{(\sqrt{K_c B} + \gamma)^2} \times \left. \frac{\partial \sqrt{K_c B}}{\partial w} \right|_\gamma dw = \Pi_\gamma N dw \quad (13)$$

so that the consequence of a tension γ on surface pressure is,

$$\Pi_\gamma = -\gamma \left. \frac{kT}{8\pi N} \frac{q_{\text{Max}}^2}{(\sqrt{K_c B} + \gamma)^2} \frac{\partial \sqrt{K_c B}}{\partial w} \right|_\gamma \quad (14)$$

This extra contribution is small for very large γ because at large γ there is very little surface undulation, A_c itself has gone to zero with the progressive tightening of the multilayer as it was brought from zero to high tension. (If the undulation-free multilayer surface were itself curved, with a radius r , as with an “onion-form” liposome rather than the flat multilayer analyzed here, there would also be an osmotic Laplace pressure analogous to $p_L = 2\gamma/r$.)

Recall now the excursions in A_c vs w in Fig. 17 and see immediately how surface energy creates a Π_γ that adds to or subtracts from the osmotic stress experimentally applied to the multilayer. This is an instructive way to view the plots in Fig. 20.

We have not explained the paradox. We have suggested a strategy by which it might be examined and have shown how properties of lamellar geometry impart sensitivity to system parameters that have been hard to control. In this vein it is essential to recognize the large assumptions made in this first, mean-field model where bilayer spacing is assumed uniform. For very thick multilayers or layers under strong surface perturbation, spacing can be expected to be non-uniform.

We have used as a material property the compressibility $B(w)$ measured on multilayers in which undulations are already occurring. We are making believe that the additional, tension-effected work of compressing and bending the layers in this already-undulating system can be described in terms of a Hamiltonian that begins with hypothetically flat layers.

Following conventions in osmotic stress measurements, we have ascribed all the water-volume change to changes in water spacing with little

added contribution from lipid bilayer contour. In this sense, we are restricted to situations where ripples are small, $A_c \ll 1$. This is because the measured $\Pi_{osmotic}(w)$ curves of multilayers in water use stoichiometric measurements of the volume of water, $w = w(V_w)$ so that w is in fact the variable used to calibrate the volume of water. Complete solution of the “inverse problem”, beginning with flat layers and direct interactions, would re-define w ; changes in water volume would be written as functions of bilayer separation and contour area.

In principle, the mean-field perturbation picture will work only for small perturbations. That restriction can be violated when we use the $\gamma = 0$ limit as a reference state. Having recognized this limitation, we would like the results given here to be taken only as qualitative indications of the direction of change with application of finite γ . Regions of instability are particularly likely to appear different when treated more rigorously. We are happy now simply to have seen this unexpected instability and are working on the necessary next step.

We are left with this. The flexibility of large molecules is intrinsic to their organization. Any long-range effect of surfaces on molecular packing immediately leads to a troubling question. Do the laws of molecular organization observed in cm-sized test tubes hold within the confines of micrometer sized cells, viruses or colloids? Only by continuing to examine – by experiment and theory – the effects of surfaces will we see why dramatic consequences come from seemingly small differences in preparation.

Acknowledgment

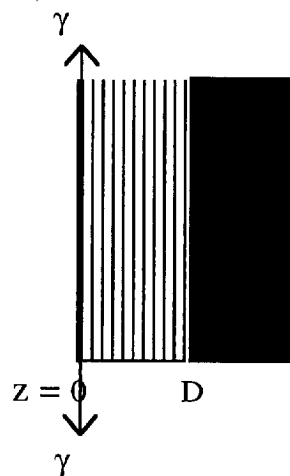
This paper is dedicated to Barry Ninham as a 60th birthday gift. The fact that it deals with a mechanical version of van der Waals forces brings to one of us (V.A.P.) many happy memories of ardently working with Barry through similar concepts almost thirty years ago. We thank Peter Deusing, Sol Gruner, Per Lyngs Hansen, Sergey Leikin and Peter Rand for perceptive criticism and suggestions. P.L.H. pointed out to us L.V.

Mikheev’s prescient paper late in the preparation of this manuscript.

Appendix

Modal expansion of undulations

We examine the action of surface tension γ on an N -layer multilayer of thickness D deposited on a solid surface, one surface under tension,



En face, the sample has the lateral dimension $L \times L$ of a square.

Inside the multilayer, there is an energy density given by a bulk Hamiltonian H_{bulk} of compressive, B , and bending K_c terms,

$$H_{bulk} = 1/2 \{ B(\partial u / \partial z)^2 + K_c ((\partial^2 u / \partial \rho^2)^2) \} \tag{A1}$$

The energy is given in terms of a local displacement of the layers perpendicular (z -direction) to the mean layer plane: $u = u(x, y, z)$ and $x^2 + y^2 = \rho^2$. This energy density H_{bulk} is to be integrated over the full volume. The modulus B has the units of an inverse compressibility. We will use the measured osmotic stress $\Pi_{osm}(w)$ vs water separation w between bilayers of a multilayer in liquid solution to give us,

$$B = B(w) \equiv -w(\partial \Pi_{osm}(w) / \partial w) \tag{A2}$$

with units of energy per volume.

The bulk bending modulus,

$$K_c \equiv k_c / w \tag{A3}$$

where k_c is the bending modulus of a single layer with units of energy so that K_c is in energy/length.

To the bulk energy density we add a tension term wherein the applied lateral tension γ at the surface acts on the rippling contour $s(x,y,z)$ of the surface. This rippled area is greater than the flat planar area by an amount $(ds^2 - d\rho^2)$ at each position ρ with,

$$(ds)^2 = [1 + (\partial u / \partial \rho)^2](d\rho)^2; \quad ds \approx [1 + (1/2)(\partial u / \partial \rho)^2]d\rho \quad (A4)$$

evaluated at $z=0$. A change in surface tension $d\gamma$ changes the free energy by an amount,

$$H_{\text{surface}} = (1/2)(\partial u / \partial \rho)^2 d\gamma \quad (A5)$$

integrated over the full surface.

We expand $u(x,y,z)$ in fourier series, modes or waves in the x,y plane penetrating in the z direction:

$$u(x,y,z) = \sum_q u_q(z) e^{iq\rho} \quad (A6)$$

where $u_q(z)$ is the fourier transform of $u(x,y,z)$ for the radial vector q in the x and y direction.

Since the sample has finite boundaries, there is a lowest non-zero wave vector $q_{\text{min}} \sim \pi/L$ corresponding to a wavelength twice the dimensions of the sample.

H_{bulk} can be expressed as a sum of fourier components in the form,

$$B u_q'(z)^2 + K_c q^4 u_q(z) \quad (A7)$$

The solution for $u_q(z)$ comes from minimizing this quantity integrated over z using a Euler-Lagrange condition,

$$d/dz[(\partial/\partial u_q')] = (\partial/\partial u_q) \quad (A8)$$

to get the differential equation,

$$B u_q''(z) = K_c q^4 u_q(z) \quad (A9)$$

For each q contribution there is a natural length from the ratio of $\sqrt{B/K_c q^4}$ (This is because B is in energy/length³, K_c in energy/length and q^4 in 1/length⁴.) The displacement function $u_q(z)$ will necessarily be a function of the product,

$$\sqrt{\frac{K_c}{B}} q^2 z \equiv a_q z \quad (A10)$$

In general,

$$u_q(z) = A_q \exp(-a_q z) + B_q \exp(a_q z) \quad (A11)$$

It is clear that fluctuations corresponding to small a_q will extend further in the z direction perpendicular to the surface. For each mode q , with this form for $u_q(z)$, we write down the modal energy as the sum of bulk and surface energies.

The bulk Hamiltonian gives the energy inside the $L \times L \times D$ multilayer,

$$K_c q^4 L^2 \int_0^D d[A_q^2 \exp(-2a_q z) + B_q^2 \exp(2a_q z)] \\ = \frac{1}{2} \sqrt{K_c B} q^2 L^2 [A_q^2 (1 - \exp(-2a_q D)) \\ + B_q^2 (\exp(2a_q D) - 1)] \quad (A12)$$

The surface Hamiltonian gives an energy that is the excess surface area times γ ,

$$\frac{1}{2} q^2 L^2 [A_q^2 \exp(-2a_q z) + 2A_q B_q + B_q^2 \exp(2a_q z)] \gamma \\ = \frac{1}{2} q^2 L^2 [A_q + B_q]^2 \gamma \quad (A13)$$

We use boundary conditions to eliminate B_q , to write the modal energy E_q as a function only of the unknown A_q in the Hookean form,

$$E_q = (1/2) K_H A_q^2 \quad (A14)$$

By standard methods, the modal free energy,

$$G_q = (kT/2) \ln K_H \quad (A15)$$

The magnitude of A_q is found from the equipartition theorem requiring that $E_q = kT/2$.

For a multilayer adhering to a solid substrate, $u_q(z=D) = 0$,

$$B_q = -A_q \exp(-2a_q D) \quad (A16)$$

The undulation profile across thickness z is then,

$$u_q(z) = A_q \exp(-a_q z) - A_q \exp(-2a_q D) \cdot \exp(a_q z) \\ = A_q [\exp(-a_q z) - \exp(-2a_q D) \exp(a_q z)] \quad (A17)$$

The modal energy E_q is,

$$E_q = \frac{1}{2} \{ \sqrt{K_c B} [1 - \exp(-4a_q D)] + [1 - \exp(-2a_q D)]^2 \gamma \} q^2 L^2 A_q^2 \quad (A18)$$

and

$$A_q^2 = kT / [\{ \sqrt{K_c B} [1 - \exp(-4a_q D)] + [1 - \exp(-2a_q D)]^2 \gamma \} q^2 L^2] \quad (A19)$$

From this quadratic form for E_q , ignoring γ -independent terms, we have the modal free energy,

$$G_q = \frac{kT}{2} \ln \{ \sqrt{K_c B} [1 + \exp(-2a_q D)] + [1 - \exp(-2a_q D)] \gamma \} \quad (A20)$$

For large multilayer thickness D , modal energy E_q and free energy G_q go to,

$$E_q = \frac{1}{2} \{ \sqrt{K_c B} + \gamma \} q^2 L^2 A_q^2 \quad (A21)$$

and

$$G_q = \frac{kT}{2} \ln \{ \sqrt{K_c B} + \gamma \} \quad (A22)$$

$$A_q^2 = kT / [\{ \sqrt{K_c B} + \gamma \} q^2 L^2] \quad (A23)$$

Integration over modes q – free energy

The goal is to see what happens to the free energy G when we change applied osmotic stress Π_{osm} and surface energy γ ,

$$dG(\Pi_{osm}, \gamma) = (\partial G / \partial \Pi_{osm}) d\Pi_{osm} + (\partial G / \partial \gamma) d\gamma \quad (A24)$$

$$dG(\Pi_{osm}, \gamma) = V_w(\Pi_{osm}, \gamma) d\Pi_{osm} + A_{total}(\Pi_{osm}, \gamma) d\gamma \quad (A25)$$

$V_w(\Pi_{osm}, \gamma)$ and $A_{total}(\Pi_{osm}, \gamma)$ are, respectively, the volume of water and the total contour area of the adsorbed multilayer (as described under Section 2).

The excess area for each q is the derivative $(\partial G_q / \partial \gamma)$,

$$\begin{aligned} (\partial G_q / \partial \gamma) |_{\Pi} &= A_q = \frac{kT}{2} \frac{[1 - e^{-2a_q D}]}{\{ \sqrt{K_c B} [1 + e^{-2a_q D}] + [1 - e^{-2a_q D}] \gamma \}} \rightarrow \frac{kT}{2} \frac{1}{\{ \sqrt{K_c B} + \gamma \}} \end{aligned} \quad (A26)$$

³We want to compute the shrinkage of the multilayer from the wave-stilling action of surface energy γ . The desired relation, $(\partial V_w / \partial \gamma)$, can be obtained from a Maxwell cross relation,

$$(\partial V_w / \partial \gamma) |_{\Pi} = (\partial A_{total} / \partial \Pi_{osm}) |_{\gamma} \quad (A27)$$

It is because we will be taking this $(\partial A_{total} / \partial \Pi_{osm}) |_{\gamma}$ derivative after the derivative $(\partial G / \partial \gamma)$ that we can afford to ignore the flat-surface energy γL^2 as well as γ -independent terms in G . In practice the required derivative is to be taken with respect to the bulk property $\sqrt{K_c B}$ with a subsequent derivative – numerically, on the measured function – $(\partial \sqrt{K_c B} / \partial \Pi)$.

The area $(\partial G / \partial \gamma) |_{\Phi}$ is the integral of areas A_q ,

$$A_q = \frac{kT}{2} \frac{[1 - e^{-2a_q D}]}{\{ \sqrt{K_c B} [1 + e^{-2a_q D}] + [1 - e^{-2a_q D}] \gamma \}}$$

over all q vectors as,

$$\frac{kT}{2} \int_{q_{min}}^{q_{max}} \frac{2\pi q dq}{(2\pi)^2} \frac{[1 - e^{-2a_q D}]}{\{ \sqrt{K_c B} [1 + e^{-2a_q D}] + [1 - e^{-2a_q D}] \gamma \}}$$

Recalling $\sqrt{\frac{K_c}{B}} q^2 \equiv a_q$ Eq. (A10), we have an

integral over $x = 2\sqrt{\frac{K_c}{B}} q^2 D = 2a_q D$.

$$\begin{aligned} (\partial G / \partial \gamma) &= \frac{kT}{16\pi \sqrt{\frac{K_c}{B}} D} \int_{x_{min}}^{x_{max}} dx \\ &\times \frac{[1 - e^{-x}]}{\{ (\sqrt{K_c B} + \gamma) + (\sqrt{K_c B} - \gamma) e^{-x} \}} \end{aligned}$$

³ An alternative way to see this result is to go back to E_q put in the Hookean quadratic form $E_q = (1/2) K_H A_q^2$. The modal average internal energy is $E_q = kT/2 = (1/2) K_H \langle A_q^2 \rangle$. The excess surface area is the coefficient of γ in E_q , $(1/2) [1 - \exp(-2a_q D)]^2 q^2 L^2 A_q^2$, into which we introduce $\langle A_q^2 \rangle = kT/K_H$.

$$= \frac{kT}{16\pi\sqrt{\frac{K_c}{B}}D} (I_1 + I_2) \quad (\text{A28})$$

$$I_1 = \int_{x_{\min}}^{x_{\max}} \frac{dx}{\{(\sqrt{K_c B} + \gamma) + (\sqrt{K_c B} - \gamma)e^{-x}\}}$$

$$= \int_{x_{\min}}^{x_{\max}} \frac{dx}{\{\alpha + \beta e^{-x}\}} = \frac{x_{\max} - x_{\min}}{\alpha}$$

$$+ \frac{1}{\alpha} \ln\left(\frac{\alpha + \beta e^{-x_{\max}}}{\alpha + \beta e^{-x_{\min}}}\right)$$

$$I_2 = \int_{x_{\min}}^{x_{\max}} \frac{-e^{-x} dx}{\{(\sqrt{K_c B} + \gamma) + (\sqrt{K_c B} - \gamma)e^{-x}\}}$$

$$= \int_{x_{\min}}^{x_{\max}} \frac{-e^{-x} dx}{\{\alpha + \beta e^{-x}\}} = \frac{1}{\beta} \ln\left(\frac{\alpha + \beta e^{-x_{\max}}}{\alpha + \beta e^{-x_{\min}}}\right)$$

We look at the limit where $x_{\max} \gg x_{\min}$ and $x_{\min} \approx 0$, then

$$\left. \frac{\partial G}{\partial \gamma} \right|_{\Pi_{\text{osm}}} = \frac{kT}{16\pi\sqrt{\frac{K_c}{B}}D} \frac{2\sqrt{\frac{K_c}{B}}Dq_{\max}^2}{\sqrt{K_c B} + \gamma}$$

$$+ \frac{kT}{16\pi\sqrt{\frac{K_c}{B}}D} \frac{\ln\left(\frac{\sqrt{K_c B} + \gamma}{2\sqrt{K_c B}}\right)}{\sqrt{K_c B} + \gamma}$$

$$+ \frac{kT}{16\pi\sqrt{\frac{K_c}{B}}D} \frac{\ln\left(\frac{\sqrt{K_c B} + \gamma}{2\sqrt{K_c B}}\right)}{\sqrt{K_c B} + \gamma}$$

$$= \frac{kT}{8\pi} \frac{q_{\max}^2}{\sqrt{K_c B} + \gamma}$$

$$+ \frac{kT}{8\pi DK_c} \frac{\ln\left(\frac{1 + \gamma/\sqrt{K_c B}}{2}\right)}{1 - (\gamma/\sqrt{K_c B})^2} \quad (\text{A29})$$

The second term is much smaller than the first.

The γ -dependent factor in the second term is on the order of 1 or less. The quantity in the denominator $DK_c = Nwk_c/w = Nk_c$. If $N = 100$ and $k_c = 10^{-12}$ erg, typical for phospholipid bilayers, then $Nk_c = 10^{-10}$ erg.

If γ is 100 erg cm⁻², huge compared with $\sqrt{K_c B}$ (see Section 3, and $q_{\max} \sim 2\pi/30$ Å, then

$$\frac{q_{\max}^2}{\sqrt{K_c B} + \gamma} \sim 10^{13} \gg \frac{1}{DK_c} \sim 10^{10}.$$

For this reason, we will continue our discussion by using only the first term,

$$\left. \frac{\partial G}{\partial \gamma} \right|_{\Pi_{\text{osm}}} = \frac{kT}{8\pi} \frac{q_{\max}^2}{\sqrt{K_c B} + \gamma} \quad (\text{A30})$$

The dropped terms may be important in systems different from those considered in this paper.

References

- [1] L.V. Mikheev, Sov. Phys. JETP 69 (1989) 632–640.
- [2] A. Adjari, B. Duplantier, D. Hone, L. Peliti, J. Prost, J. Phys. II (France) 2 (1992) 487.
- [3] R. Podgornik and A. Parsegian, Biophys. J. 72 (1997) 942–952.
- [4] A.C. Cowley, N.L. Fuller, R.P. Rand, V.A. Parsegian, Biochemistry 17 (1978) 3163–3168.
- [5] M.E. Loosley-Millman, R.P. Rand, V.A. Parsegian, Biophys. J. 40 (1982) 221–232.
- [6] G.L. Jendrasiak, J.H. Hasty, Biochim. Biophys. Acta 337 (1974) 79.
- [7] G.L. Jendrasiak, R.L. Smith, Shaw, Biochim. Biophys. Acta 1279 (1996) 63–69.
- [8] R.P. Rand, V.A. Parsegian, Biochim. Biophys. Acta, Biomembranes Review 988 (1989) 351–376.
- [9] R.P. Rand, V.A. Parsegian, in: Structure and Dynamics of Membranes, Handbook of Biological Physics, Vol. 1b, ch. 13, 1995, pp. 643–690.
- [10] G.S. Smith, C.R. Safinya, D. Roux, N. Clark, Mol. Cryst. Liq. Cryst. 144 (1987) 235.
- [11] S. Tristram-Nagle, R. Zhang, R.M. Suter, C.R. Worthington, W.-J. Sun, J.F. Nagle, Biophys. J. 64 (1993) 1097–1109.
- [12] T.J. McIntosh, Biochemistry.
- [13] J.F. Nagle, R. Zhang, S. Tristram-Nagle, W. Sun, H.I. Petrache, R.M. Suter, Biophys. J. 70 (1996) 1419–1431.
- [14] A. Caillé, C.R. Acad. Sci., Paris B 274 (1972) 891.
- [15] G.S. Smith, E.B. Sirota, C.R. Safinya, N. Clark, J. Chem. Phys. 92 (1990) 4519.
- [16] P.M. Chaikin, T.C. Lubensky, Principles of Condensed

- Matter Physics, Cambridge University Press, Cambridge, 1995.
- [17] P-G de Gennes, J. Prost, *The Physics of Liquid Crystals*, Clarendon Press, Oxford, 1995.
- [18] B. Klösgen, W. Helfrich, *Biophys. J.* (1995) February supplement, Biophysical Society meeting abstracts.
- [19] E.A. Evans, W. Rawicz, *Phys. Rev. Lett.* 64 (1990) 2094-2097 bending moduli.
- [20] V.A. Parsegian, *Langmuir* 12 (1993) 3625–3628.
- [21] E.A. Evans, D. Needham, *J. Phys. Chem.* 91 (1987) 4219.
- [22] P. Attard, D.J. Mitchell, B.W. Ninham, *Biophys. J.* 53 (1988) 457–460.
- [23] R.P. Rand, N.L. Fuller, V.A. Parsegian, D.C. Rau, *Biochemistry* 27 (1988) 7711–7722.
- [24] W. Helfrich, *Z. Naturf.* 33a (1978) 305–315.
- [25] E. Evans, V.A. Parsegian, *PNAS* 83 (1986) 7132.
- [26] R. Podgornik, V.A. Parsegian, *Langmuir* 8 (1992) 557–562.
- [27] V.A. Parsegian, D.C. Rau, N.L. Fuller, R.P. Rand, *Meth. Enzymol.* 127 (1986) 400–416.